Journal of Electroanalytical Chemistry 763 (2016) 116–124

Contents lists available at ScienceDirect

Journal of Electroanalytical Chemistry

journal homepage: www.elsevier.com/locate/jelechem

Ethanol oxidation on shape-controlled platinum nanoparticles at different pHs: A combined in situ IR spectroscopy and online mass spectrometry study

Carlos Busó-Rogero [a], Sylvain Brimaud [b], Jose Solla-Gullon [a], Francisco J. Vidal-Iglesias [a], Enrique Herrero [a],*, R. Jürgen Behm [b], Juan M. Feliu [a]

[a] Instituto de Electroquímica, Universidad de Alicante, Apartado 99, E-03080 Alicante, Spain
[b] Institut für Oberflächenchemie und Katalyse, Universität Ulm, Albert-Einstein-Allee 47, D-89081 Ulm, Germany

ARTICLE INFO

Article history:
Received 3 October 2015
Received in revised form 19 December 2015
Accepted 22 December 2015
Available online 29 December 2015

Keywords:
Ethanol oxidation
pH effect
Platinum
Nanoparticles
DEMS

ABSTRACT

Ethanol oxidation on different shape-controlled platinum nanoparticles at different pHs was studied using electrochemical, Attenuated Total Reflection-Fourier Transform Infrared Spectroscopy (ATR-FTIR) and, especially, Differential Electrochemical Mass Spectrometry (DEMS) techniques, the latter giving interesting quantitative information about the products of ethanol oxidation. Two Pt nanoparticle samples were used for this purpose: (100) and (111) preferentially oriented Pt nanoparticles. The results are in agreement with previous findings that the preferred decomposition product depends on surface structure, with CO_{ads} formation on (100) domains and acetaldehyde/acetic acid formation on (111) domains. However, new information has been obtained about the changes in CH_x and CO formation at lower potentials when the pH is changed, showing that CH_x formation is favored against the decrease in CO adsorption on (100) domains. At higher potentials, complete oxidation to CO_2 occurs from both CH_x and CO fragments. In (111) Pt nanoparticles, the splitting of C—C bond is hindered, favoring acetaldehyde and acetate formation even in 0.5 M H_2SO_4. C1 fragments become even less when the pH increases, being nearly negligible in the highest pH studied.

1. Introduction

During the last years, the search for new energy sources has been intensified due to the depletion of fossil fuels. In this sense, fuel cell technology has gained momentum for obtaining electric energy from the oxidation of a chemical fuel [1]. In the quest for possible new fuels, several options have been considered and particularly the oxidation of some small organic molecules such as formic acid, methanol or ethanol has been extensively evaluated. The oxidation of these molecules normally requires the use of platinum as catalyst [2–4]. Among these fuels, ethanol presents some relevant advantages to other fuels as i) it can be obtained directly from biomass and ii) it does not present problems for its storage. Unfortunately, and despite its high density energy for the complete oxidation to CO_2, with 12 electrons exchanged, problems dealing with a classical CO poisoning as well as to an incomplete oxidation to undesired products such as acetic acid, limit its potentialities for practical purposes.

Ethanol oxidation is also known to be a surface structure sensitive reaction, that is, the resulting catalytic activity depends on the particular/specific arrangement of the surface atoms. This surface structure sensitivity has been clearly evidenced by the use of Pt single crystal electrodes [5–7]. However, single crystal electrodes are ideal model surfaces which cannot be used in real electrocatalytic systems. For this reason, these results have to be extended to nanoparticles, which can be effectively applied to such systems. As previously demonstrated, the effect of the particular arrangement of the atoms at the surface on the resulting ethanol oxidation activity is valid also for nanoparticles [8], thus highlighting the importance of gaining control over the surface structure of the nanoparticles to increase their electrocatalytic activity. Similar results on the effect of the surface structure of the nanoparticles for other important reactions such as oxygen reduction or other small organic molecule oxidations have been already reported [9–16]. In this sense, it is also worth noting that these shape/surface structure controlled Pt nanoparticles are usually about 8–10 nm in size which, from a practical point of view, may be insufficient to fulfill the requirement of a high surface-to-volume ratio for practical applications.

From a mechanistic point of view, it is known that, in acidic solutions the reaction occurs via a complex reaction network. The following

---

* Corresponding author.
E-mail address: herrero@ua.es (E. Herrero).

http://dx.doi.org/10.1016/j.jelechem.2015.12.034
1572-6657/© 2015 Elsevier B.V. All rights reserved.

scheme illustrates a simplified mechanism where some additional steps such as desorption and re-adsorption of acetaldehyde have not been included for the sake of clarity.

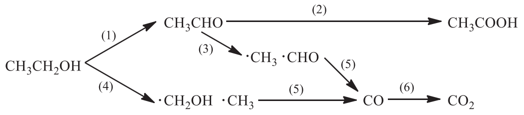

Reaction steps (1) and (2) give rise to the incomplete oxidation of ethanol, forming acetaldehyde and acetic acid as final products. To obtain this latter product, which is very difficult to oxidize, only four electrons are exchanged, thus wasting 2/3 of the formal energy density for ethanol. On Pt (111) electrodes and at room temperature, the reaction only takes place almost exclusively through this undesirable route [5]. On the other hand, the splitting of the C—C bond occurs in steps (3) and (4), which produce different carbon fragments that are subsequently transformed to CO_{ads} (step (5)) [5,17,18]. Finally, in step (6), CO_{ads} is oxidized to CO_2, thus completing the 12 electron exchange route. This reaction route presents two difficult steps, i) the splitting of the C—C bond and ii) the oxidation of adsorbed CO. Pt(110) and especially Pt(100) electrodes favor the C—C bond scission, but suffer from surface poisoning. The enhancement of the C—C bond breaking rate needs to be accompanied by a higher rate for CO_{ads} oxidation to avoid poisoning. In fact, the stronger the metal-adsorbate bond, the more C—C bond breaking is favored, while CO_{ads} oxidation is disfavored. This is likely to result in a Sabatier type behavior with an optimum bond strength. In order to overcome this CO_{ads} poisoning problem, the incorporation of different foreign atoms has been used to facilitate CO_{ads} oxidation to CO_2 [19–21]. In addition, the breakage of C—C bond is known to be improved on Pt surfaces containing (100) and (110) steps on (111) terraces [6,22]. Consequently, a combination of these two approaches, that is, using stepped Pt electrodes and foreign adatoms, gave rise to significant improvements in the oxidation reaction [17,18,20].

On the other hand, the research of alkaline fuel cells (AFC) has currently grown due to the higher activity obtained at these pHs and also due to their less corrosive properties, which favor the use of cheaper catalysts. In fact, the problems resulting from the carbonation of the system due to CO_2 retention as well as from the limited number of membranes capable of operating over long periods of time in alkaline media seem to be solved with the development of new anion-exchange membranes [23,24]. According to fundamental studies performed in alkaline solutions [7,25,26], acetate is presented as the main product for ethanol oxidation regardless of the surface structure of the Pt electrode, with negligible amounts of CO_{ads} being formed. Consequently, a better understanding of the changes in the oxidation mechanism as a function of the pH and in particular, how the ratio between the products (incomplete oxidation to acetate or complete oxidation towards CO_2) is modified for increasing pHs, would be of utmost interest.

To access this information, we have performed a combined in situ infrared (IR) spectroscopy and online mass spectrometry study on different shape controlled Pt nanoparticles of the ethanol oxidation reaction (EOR) at different pHs. These experiments will be performed under well-defined mass transport conditions and with control of the surface structure, in contrast to infrared reflection-absorption spectroscopy (IRRAS) measurements, where by-product accumulation, e.g. adsorbed acetate, is common. Such experimental conditions are more convenient for mechanistic investigations. On the other hand, it is also worth noting that only pHs lower than 4 have been explored in order to avoid problems due to carbonate formation. This combined approach allows us to not only perform a quantitative analysis of the volatile products formed during the reaction and to calculate the efficiencies for the complete oxidation to CO_2, but also to follow the nature and potential window in which the adsorbed intermediate species are formed during the reaction.

2. Experimental

Two different kinds of Pt nanoparticles were used in this work. They were both synthesized using a colloidal method [27,28], and displayed preferential (100) or (111) surface orientations. These nanoparticles were denoted as (100) Pt nanoparticles and (111) Pt nanoparticles, depending on their dominant surface structure. Experimental details about the synthesis, also including Transmission Electron Microscopy (TEM) characterization to determine their particle size and characterize their preferential shape, were previously described [29]. Very briefly, the predominant shape was cubic for (100) Pt nanoparticles and octahedral for (111) Pt ones. The particle size of both nanoparticle batches was estimated to be about 8–10 nm. The electrodes were prepared by depositing a droplet (4 μL) of the aqueous solution containing the nanoparticles on a hemispherical gold substrate, after which the electrode was protected under an Ar stream until complete solvent evaporation. Before the measurements, Pt nanoparticles were carefully cleaned by CO adsorption and subsequent stripping at potentials below 0.95 V to preserve the surface structure of the samples. The electrochemically active area of Pt nanoparticles was measured using the charge involved in the so-called hydrogen/anion adsorption/desorption region (between 0.05 V and 0.6 V) from the cyclic voltammograms recorded in 0.5 M H_2SO_4, assuming that the charge density for this region is 230 μC cm^{-2} in sulfuric acid solutions [30].

IR spectroelectrochemical probing of adsorbates and online detection of volatile reaction products were performed simultaneously using a dual thin-layer spectroelectrochemical flow-cell in which ATR-FTIR and DEMS measurements can be carried out. A more detailed description of this flow-cell configuration was previously given in [31]. In brief, the central cell is a double thin-layer flow cell, equipped with two Pt counter electrodes (a Pt gauge and a Pt wire) at the inlet and the outlet of flow cell. For electrolyte changing, two electrolyte reservoirs are available, one with the supporting electrolyte alone and one with ethanol + supporting electrolyte. The working electrode is prepared by depositing the nanoparticles on a Au film covering a Si wafer, which in turn is coupled with the flat side of a hemispherical Si prism. The Au film was prepared by electroless deposition following the procedure reported previously [32–34]. It has to be thin enough to allow the IR radiation to pass to the nanoparticles, but thick enough to be sufficiently conductive for obtaining a good electrochemical response.

In the first thin-layer compartment, the flat side of the prism was pressed via a circular tightening gasket and a Cu foil current collector against the Kel-F body of the cell, forming a thin electrolyte layer with a volume of ca. 10 μL. The electrolyte flows to the second thin-layer compartment through six capillaries. The second thin-layer compartment is connected via a porous Teflon membrane to a mass spectrometer, such that gaseous species can pass through and be detected on-line.

The in situ ATR-FTIRS experiments were performed in a BioRad FTS-6000 spectrometer equipped with a homemade reflection accessory (incident angle of 70°) and mercury cadmium telluride (MCT) detector. The resolution and the acquisition time per spectra were 4 cm^{-1} and 10 s, respectively. The spectra are presented in absorbance values, as the ratio $-\log R/R_0$, where R and R_0 are the reflectance values corresponding with the single beam spectra measured at the sample or reference potential, respectively. Negative bands in the spectra correspond with species formed at the sampling potential, whereas positive bands indicate a consumption of the species with respect to reference potential.

The DEMS setup is explained in detail in ref. [35]. Briefly, it is based on a differentially pumped two-chamber system coupled with a Balzers QMS 12 quadrupole mass spectrometer, a Pine Instruments potentiostat and a computerized data acquisition system. In all the mass spectrometry experiments, large Pt loadings were used to favor the performance of DEMS experiments.

The calibration constant for CO_2 was determined by passing a CO saturated solution at 0.1 V until the Pt surface is completely blocked. Then, the electrolyte is changed to CO-free supporting electrolyte for